ELSEVIER

Polymer 43 (2002) 2261–2266

polymer

www.elsevier.com/locate/polymer

Space charge behaviors of low-density polyethylene blended with polypropylene copolymer

Chao Zhang[a,*], Teruyoshi Mizutani[a], Kazue Kaneko[a], Tatsuo Mori[a], Mitsugu Ishioka[b]

[a]*Department of Electrical Engineering, Nagoya University, Furo-Cho, Chikusa-Ku, Nagoya 464-8603, Japan*
[b]*Japan Polychem Co., Kawasaki 210-0865, Japan*

Received 4 July 2001; received in revised form 8 November 2001; accepted 7 December 2001

Abstract

In this study, the space charge behaviors of the blend polymers of low-density polyethylene (LDPE) and polypropylene copolymer were investigated by the pulsed electro-acoustic method (PEA) with the electrode system of aluminium/specimen/semiconductive layer. The blend specimen composed by 90 wt% LDPE and 10 wt% polypropylene copolymer (B10) showed a larger amount of space charge than pure LDPE (PE) under a DC field of 50 MV m^{-1} at both 30 and 60 °C. Positive carriers moved more slowly in B10 than in PE under a positive DC voltage applied to the semiconductive electrode at 30 °C. DC currents were also measured under the same experimental condition as the space charge measurement. The DC current of B10 was lower than that of PE at 30 °C, but higher at 60 °C. The experimental results were explained by the introduction of traps by blending.

Keywords: Low-density polyethylene; Blend; Space charge

1. Introduction

Low-density polyethylene (LDPE) has been widely used as power cable insulation. Further improvement of electrical properties of LDPE is required to develop higher-performance cables. Blend is one of the ways to get higher-performance insulating polymers [1–3]. In our previous work, the effects of blending the random copolymer of ethylene and propylene (EP) on electrical breakdown of LDPE were investigated [3,4]. We found that the impulse breakdown strength of LDPE in the high temperature region was improved by blending with EP, and it increased with an increasing content of EP.

It is well known that the space charge strongly affects electrical conduction, breakdown and degradation process of insulating polymers [5–8]. Therefore, it is important to clarify the space charge behaviors in insulating polymers, and the relationship between space charge and inherent properties of insulating polymers. The formation of space charge in polymers, especially in polyethylene, has been extensively studied in recent years [9,10]. However, a lot of things remain unknown because of complex space charge behaviors, which are affected by many factors, such as composition, morphology, additives, and impurities of insulating polymers.

The space charge behaviors of blend polymers of polyethylene and ionomer were studied by Suh et al. [11]. However, no research on space charge of polyolefine blends was reported. In the present study, the space charge behaviors of blend polymer of LDPE and EP were investigated by the pulsed electro-acoustic method (PEA) [12], and the effect of blend of EP on space charge behavior of LDPE was discussed. The electrical conduction properties were also studied. It is important to study the space charge and conduction of polyolefine blends because polyolefine blends are usually used in practical productions. The mechanism of accumulation of space charge was discussed on the basis of the experimental results of both space charge distribution and DC current.

2. Experimental

2.1. Specimens

LDPE and EP used in this study were free from any additives. LDPE was produced with the high-pressure process. EP was copolymer of ethylene and propylene with the ethylene content of 4.5 wt%. They were originally in the form of extruded pellets. The densities of the pellets

* Corresponding author. Tel.: +81-52-789-4440; fax: +81-52-789-2698.
E-mail address: c-zhang@ieee.org (C. Zhang).

0032-3861/02/$ - see front matter
PII: S0032-3861(01)00807-2

Table 1
Specimens

Specimen	Composition	Density (g cm^{-3})	Melting point (°C)
PE	LDPE	0.916	109.5
B10	LDPE + 10 wt% EP	0.914	109.8

were 0.920 and 0.898 g cm^{-3} for LDPE and EP, respectively. Two kinds of specimens were used in this study, one was pure LDPE and the other was the blend polymer of LDPE and EP with 90 wt% LDPE and 10 wt% EP. Their films were prepared by T-die method with thickness of about 100 μm. They were called PE and B10, respectively. Their densities and melting points are listed in Table 1.

2.2. Measurements of space charge and DC current

Space charge in a specimen was measured by the PEA method, which is one of the most popular nondestructive techniques used to directly determine the space charge distribution in solid dielectrics. The principle of the method is briefly outlined as follows (see Ref. [12] for its details). An electric pulse voltage together with a high DC voltage is applied to a specimen sandwiched between upper electrode and lower electrode. Then, acoustic waves are generated by the charges on the electrode and in the bulk. The acoustic waves propagate in both directions, and are converted into electric signals by a piezoelectric transducer located at the back of the lower electrode. The position of charge can be determined by the responded reach time of the signal while the amount of charge is obtained from the magnitude of the signal. Thus, the charge distribution is reflected by the signals. Fig. 1 shows the schematic diagram of PEA used in this study.

In the present study, a film specimen is set between a semiconductive electrode (upper electrode) and an aluminium electrode (lower electrode, ground). The polyvinylidenefluoride film is employed as a piezoelectric transducer.

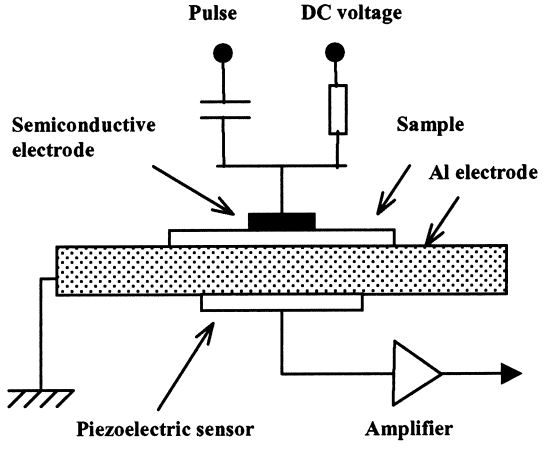

Fig. 1. Schematic diagram of PEA for the measurement of space charge distribution.

Positive or negative DC voltages are applied to the semiconductive electrode (referred to positive polarity or negative polarity, respectively) for 90 min, and then the specimen is short-circuited for another 90 min. The space charge profiles were measured at 30 and 60 °C.

The DC current was also measured under the same condition as the measurement of space charge distribution.

3. Results and discussion

3.1. Space charge distribution at 30 °C

Typical results of space charge distributions in specimens under a DC field of 50 MV m^{-1} for the positive polarity at 30 °C are shown in Fig. 2. Positive carriers are injected from the semiconductive electrode into PE (see Fig. 2(a)). The amount of positive space charge increases with time in the first 20 min after the application of DC voltage, and then it tends to saturate (see Fig. 2(b)). In the case of B10, positive carriers are also injected from the semiconductive electrode (see Fig. 2(c)). The amount of positive space charge increases with time in the first 10 min, and then it decreases as shown in Fig. 2(d). The front of positive space charge arrives at the counter aluminium electrode in about 3 min for B10, but in 1 min for PE. This suggests that the migration of positive space charge is much faster in PE than in B10. Furthermore, the amount of positive space charge in B10 is much greater than that in PE.

Fig. 3 shows the space charge distributions in specimens at 50 MV m^{-1} for the negative polarity at 30 °C. In PE, positive carriers injected from the aluminium electrode are observed, and the front of positive space charge arrives at the semiconductive electrode within 1 min. Negative carriers are also injected from the semiconductive electrode as shown in Fig. 3(a). After 2 min, positive space charge starts to decrease, and disappears at about 20 min (see Fig. 3(b)). After 20 min, only negative space charge is observed, and the amount of negative space charge increases with time. These results suggest that the positive carriers move faster than negative carriers in PE, but the amount of positive carriers injected from the aluminium electrode is less than that of negative carriers injected from the semiconductive electrode. On the other hand, positive carriers injected from the aluminium electrode and negative carriers injected from the semiconductive electrode are observed in B10 (see Fig. 3(c)). Both positive and negative space charges decrease from about 20 min (see Fig. 3(d)). The amount of space charge in B10 is much greater than that in PE.

3.2. Space charge distribution at 60 °C

Fig. 4 shows the typical space charge distributions in specimens at 50 MV m^{-1} for the positive polarity at 60 °C. In PE, positive space charge is observed in whole specimen soon after the application of DC voltage, it decreases with time, and almost disappears at 90 min as

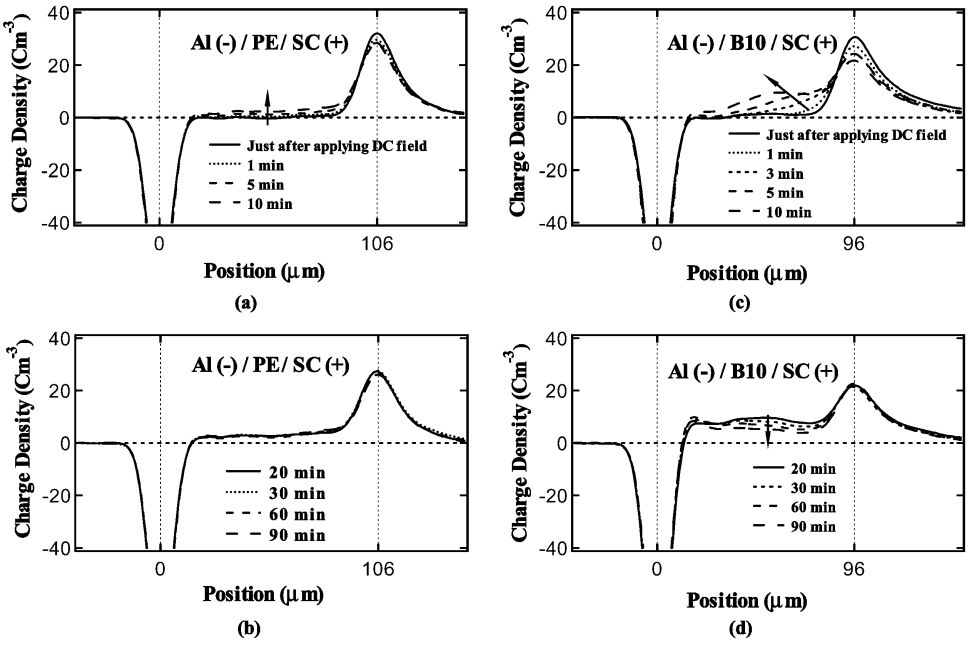

Fig. 2. Space charge distributions under a DC field of 50 MV m^{-1} for positive polarity at 30 °C. (a) PE (0–10 min), (b) PE (20–90 min), (c) B10 (0–10 min), (d) B10 (20–90 min).

shown in Fig. 4(a). This result is consistent with the previous paper [9]. In B10, the space charge distribution soon after the application of voltage at 60 °C is similar to those profiles at 20–90 min at 30 °C. This is related to carriers moving faster in high temperature. The positive space charge decreases with time after 2 min. The negative space charge appears after 10 min and increases with time. Its majority is found in the vicinity of the semiconductive electrode (anode). B10 has a larger space charge than PE.

Fig. 5 shows the space charge distributions in specimens at 50 MV m^{-1} for the negative polarity at 60 °C. Although the amount of space charge in PE is very small at 60 °C, it is

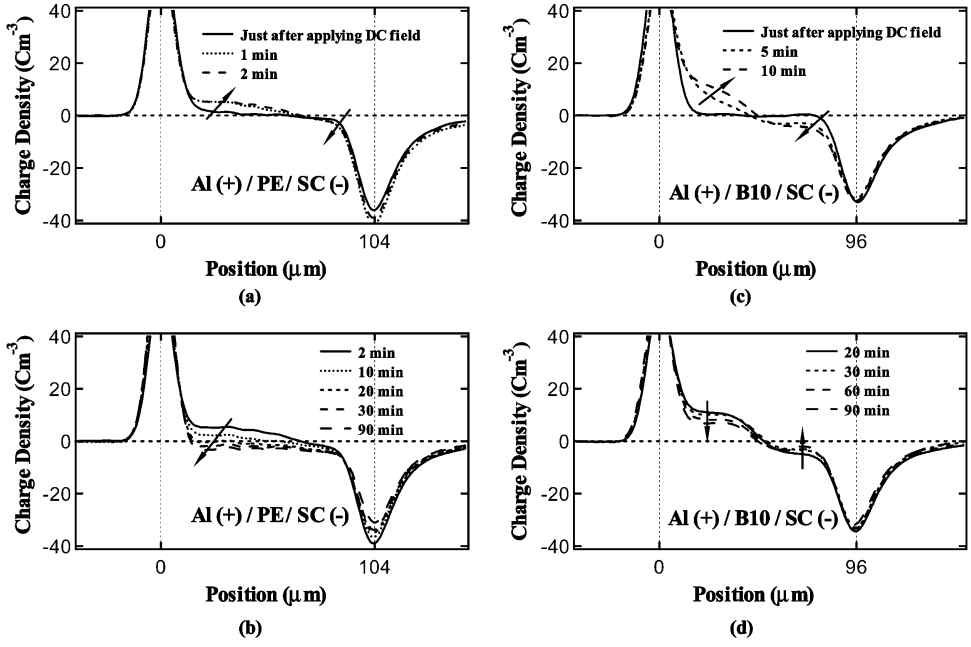

Fig. 3. Space charge distributions under a DC field of 50 MV m^{-1} for negative polarity at 30 °C. (a) PE (0–2 min), (b) PE (2–90 min), (c) B10 (0–10 min), (d) B10 (20–90 min).

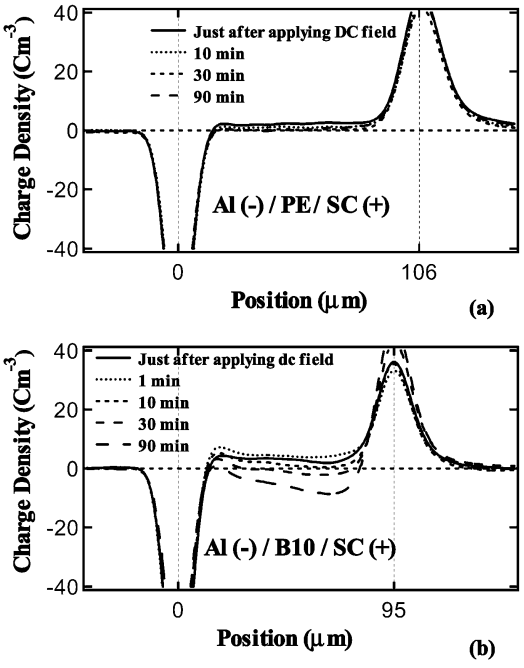

Fig. 4. Space charge distributions under a DC field of 50 MV m^{-1} for positive polarity at 60 °C. (a) PE, (b) B10.

found that positive carriers are injected from the aluminium anode and negative carriers are injected from the semiconductive cathode as shown in Fig. 5(a). B10 has negative space charge in the vicinity of the aluminium electrode, and positive space charge in the bulk and the vicinity of the semiconductive electrode as shown in Fig. 5(b). Both negative and positive space charges increase with time under the application of voltage, and the amount of positive charge is larger than that of negative one. B10 has much larger space charge than PE at 60 °C.

3.3. DC current

Typical time dependence of charging currents for PE and B10 under a DC field of 50 MV m^{-1} at 30 °C are shown in Fig. 6. PE shows a higher current than B10 at 50 MV m^{-1} for both polarities. No obvious difference in charging currents of PE can be found between the positive polarity and the negative polarity. The charging current of PE decreases with time and reaches the steady state in about 70 min after the voltage application. In B10, charging currents for the positive polarity is greater than that for the negative polarity, but they have a similar trend. They decrease during the first 15–20 min, and then turn to increase slowly with time.

Fig. 7 shows charging current versus time characteristics for PE and B10 at 60 °C. There is no clear difference in charging currents between the positive polarity and the negative polarity for both PE and B10. The charging current of PE decreases with time in the first 15 min after the voltage application, and then increases with time. On the other hand, the charging current of B10 decreases in about 5 min, and then turns to increase. B10 has a higher charging current than PE except for in the first 2 min of charging.

Two mechanisms can be used to explain the increase of charging current during the application of DC voltage. One is Joule effect by which DC current causes Joule heating

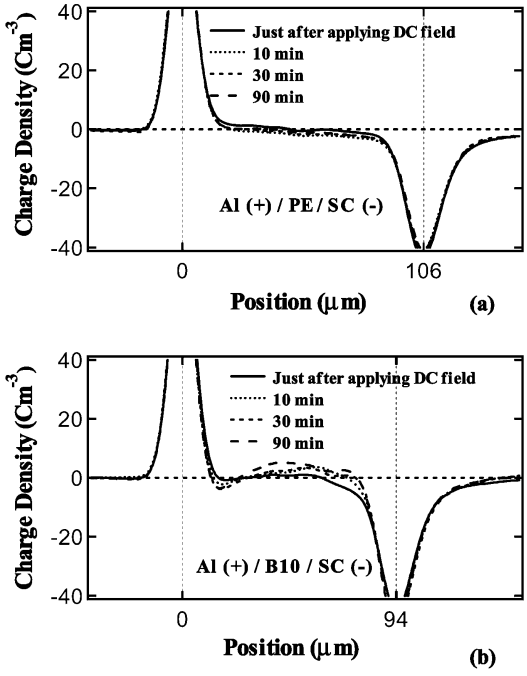

Fig. 5. Space charge distributions under a DC field of 50 MV m^{-1} for negative polarity at 60 °C. (a) PE, (b) B10.

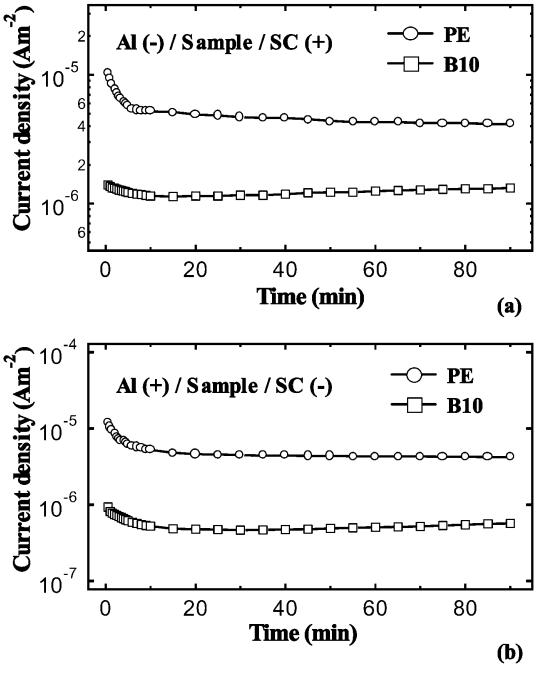

Fig. 6. Charging currents under a DC field of 50 MV m^{-1} at 30 °C for (a) positive polarity and (b) negative polarity.

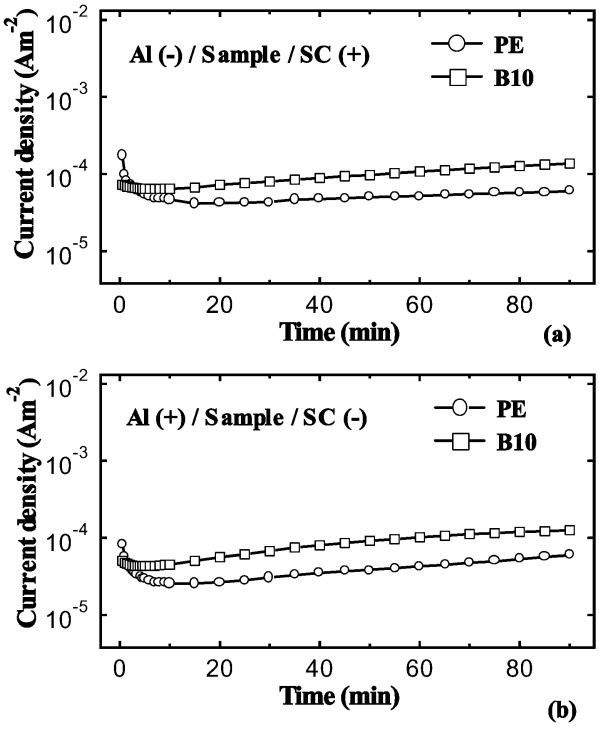

Fig. 7. Charging currents under a DC field of 50 MV m^{-1} at 60 °C for (a) positive polarity and (b) negative polarity.

during the application of DC voltage, and as a result, raises the temperature of the specimen and DC current [13]. Another is that the current is affected by space charge because space charge can distort the electric field. The charging current of PE in this experiment is explained by the former but not by the latter because space charge distributions tend to constant 20 min after the application of DC voltage at both 30 and 60 °C (see Figs. 2(b) and 4(a)). The charging current of PE does not increase at 30 °C because of a small current and heat loss due to thermal conduction. The current increase at 60 °C is explained by Joule heating. On the other hand, the charging current of B10 increases during the application of DC voltage at 30 °C because of the decrease of space charge (see Fig. 2(d)) which can result in the increase of anode field. Carriers injected from the anode are thought to be dominant because only positive space charge is observed in this case. The charging current of B10 at 60 °C may be affected by both the mechanisms.

Fig. 8 shows the plot of ln J versus $1/T$ for PE and B10, where J is the isochronal current density measured at 90 min after the application of positive DC voltage (50 MV m^{-1}), and T is the temperature. The plot of ln J versus $1/T$ shows a good straight line for both PE and B10 in the temperature range of 40–60 °C. It indicates that the current density J obeys the Arrhenius relation in this temperature range [14,15]:

$$J = A \exp[-H/(kT)], \quad (1)$$

where k, H, and A are Boltzmann constant, the thermal

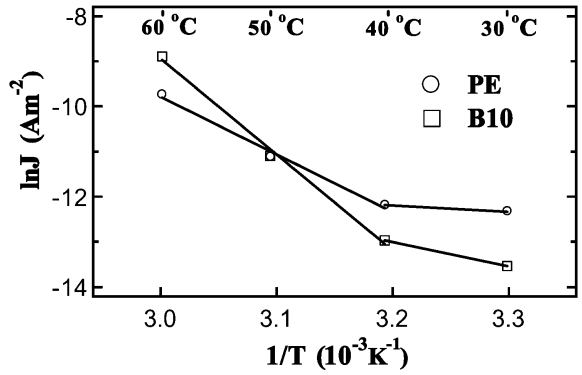

Fig. 8. Isochronal current density (J) for positive polarity as a function of reciprocal temperature ($1/T$).

activation energy, and a constant, respectively. The slopes of the straight lines give about 1.1 and 1.8 eV for PE and B10, respectively. The value of 1.1 eV for PE is close to the reported value [15,16]. However, the current values at 30 °C do not fall in these fitting lines for both PE and B10, and they show relatively higher values. Assuming a linear relationship between ln J and $1/T$ in the temperature range of 30–40 °C, the thermal activation energy can be calculated from its slope. The results are 0.1 and 0.5 eV for PE and B10, respectively. All these results suggest that B10 has higher thermal activation energies than PE.

3.4. Effects of blend on space charge and DC current

According to the experimental results mentioned earlier, the differences in space charge and DC current between PE and B10 are summarized as follows:

1. B10 has much larger space charge than PE.
2. Positive carriers move faster in PE than in B10.
3. Charging current of PE at 30 °C is higher than that of B10. On the contrary, the charging current of PE at 60 °C is lower than that of B10.
4. B10 has a higher thermal activation energy than PE.

Carrier trapping is considered to be closely related to space charge, but its details are still poorly understood [17–22]. In this paper, we assume that the differences in space charge and DC current between PE and B10 are due to the introduction of trap sites by the blend of EP. Then, the experimental results may be explained as follows.

First, injected carriers are easily trapped in B10 because of the higher density of trap sites. This results in a larger amount of space charges in B10.

Second, positive carriers move more slowly in B10 than in PE because of the suppression of mobility by trapping.

Third, the traps suppress the charging current in the room temperature region, whereas they may act as hopping sites in the high temperature region and enhance the charging current. This is a possible reason why the charging current

of B10 is lower than that of PE at 30 °C, while higher at 60 °C as shown in Figs. 6 and 7.

The carrier trapping has been studied a lot for a long time [17–22]. In general, the carrier trapping is thought to occur at boundaries of crystalline and amorphous, chain branches, local density fluctuations, impurities and so on [18]. However, practical insulating polymers have complicated physical/chemical structures and various impurities. It is difficult to clarify the correlation between solid structure and trap sites.

In the blend polymer of LDPE and EP, trap sites may be introduced in the interface region of LDPE and EP. In addition, blending of LDPE with EP will change the morphology of LDPE. In the previous work, we found that blending LDPE with EP resulted in the decrease of spherulite size and the enhancement of orientation [23]. The morphological change may also affect trap sites. However, it is difficult to determine which reason mentioned earlier is dominant in this study at the present time. Therefore, further discussion about trap sites will not be done in this paper.

4. Conclusions

We have studied the space charge behaviors and DC current properties of the blend polymers of LDPE and EP. The amount of space charge increases by blending under the application of DC voltages at 30 and 60 °C. The charging current is suppressed by blending at 30 °C, but enhanced at 60 °C. The experimental results can be explained in terms of the introduction of trap sites by blending. However, the details about trap sites are not clear and they remain under a future study.

References

[1] Kato H, Simoura S, Kawahigashi M. Proceedings of the Fourth International Conference on Properties and Applications of Dielectric Materials, Brisbane, Australia, 1994. p. 172–4.
[2] Greenway GR, Vaughan AS, Moody SM. Proceedings of 1999 Annual Report Conference on Electrical Insulation and Dielectric Phenomena, Austin, Texas, 1999. p. 666–9.
[3] Zhang C, Mori T, Mizutani T, Ishioka M. Trans IEE Jpn 2001;121-A(3):218–23.
[4] Zhang C, Mori T, Mizutani T, Ishioka M, Cheng Y. J Polym Sci, Part B: Polym Phys 2001;39(15):1741–8.
[5] Mizutani T. IEEE Trans Dielectr Electr Insul 1994;1(5):923–32.
[6] Mudarra M, Calleja RD, Belana J, Canadas JC, Diego JA, Sellares J, Sanchis MJ. Polymer 2001;42(4):1647–51.
[7] Suzuoki Y, Muto H, Mizutani T, Ieda M. J Phys D: Appl Phys 1985;18:2293–302.
[8] Dissado L, Mazzanti G, Montanari GC. IEEE Trans Dielectr Electr Insul 1997;4(5):496–506.
[9] Mizutani T, Semi H, Kaneko K. IEEE Trans Dielectr Electr Insul 2000;7(4):503–8.
[10] Wang X, Yoshimura N, Murata K, Tanaka Y, Takada T. J Appl Phys 1998;84(3):1546–50.
[11] Suh KS, Damon D, Tanaka J. IEEE Trans Dielectr Electr Insul 1995;2(1):1–11.
[12] Takada T. IEEE Trans Dielectr Electr Insul 1999;6(5):519–47.
[13] Zhang C, Kaneko K, Mizutani T. Appl Phys Lett 2001;79(23):3839–41.
[14] Mizutani T, Ieda M. IEEE Trans Electr Insul 1986;21(6):833–9.
[15] Taylor DM, Lewis TJ. J Phys D: Appl Phys 1971;4:1346–57.
[16] Mizutani T, Suzuoki Y, Hanai M, Ieda M. Jpn J Appl Phys 1982;11:1639.
[17] Mizutani T. J Electrostat Jpn 1995;19(5):350–7.
[18] Seanor DA. Electrical properties of polymers. New York: Academic Press, 1982. Chapter 1.
[19] Guarrotxena N, Vella N, Toureille A, Millan J. Polym Int 1998;46(1):65–71.
[20] Montanari GC. IEEE Trans Dielectr Electr Insul 2000;7(3):309–15.
[21] Dissado L, Mazzanti G, Montanari GC. IEEE Trans Dielectr Electr Insul 1995;2(6):1147–58.
[22] Lampert MA, Mark P. Current injection in solids. New York: Academic Press, 1970. Chapter 2.
[23] Zhang C, Mori T, Mizutani T, Ishioka M. Proceedings of the 32nd Symposium on Electrical and Electronic Insulating Materials and Applications in Systems. IEE Japan, 2000. p. 215–18.